Status of the benchmark activity of ICRF full-wave codes within EUROfusion WPCD and beyond

R. Bilato', N. Bertelli, M. Brambilla, R. Dumont, E. F. Jaeger, T. Johnson, E. Lerche, O. Sauter, D. Van Eester, and L. Villard

Citation: AIP Conference Proceedings **1689**, 060001 (2015); doi: 10.1063/1.4936499
View online: http://dx.doi.org/10.1063/1.4936499
View Table of Contents: http://aip.scitation.org/toc/apc/1689/1
Published by the American Institute of Physics

Status of the benchmark activity of ICRF full-wave codes within EUROfusion WPCD and beyond

R. Bilato[1,a)], N. Bertelli[2], M. Brambilla[1], R. Dumont[3], E.F. Jaeger[4], T. Johnson[5], E. Lerche[6], O. Sauter[7], D. Van Eester[6] and L. Villard[7]

[1] *MPI for Plasma Physics, 85748 Garching, Germany*
[2] *Princeton Plasma Physics Laboratory, Princeton, NJ 08543 USA*
[3] *CEA, IRFM, F-13108 Saint-Paul-lez-Durance, France*
[4] *XCEL Engineering Inc, 1066 Commerce Park Drive, Oak Ridge, Tennessee 37830, USA.*
[5] *School of Electric Engineering, KTH, Association VR-Euratom, Sweden*
[6] *Ecole Royale Militaire, Renaissancelaan 30, B-1000, Brussels, Belgium*
[7] *CRPP, EPFL, Lausanne, Switzerland*

[a)]Corresponding author: roberto.bilato@ipp.mpg.de

Abstract. As follow-up of the benchmark activity of ICRF full-wave codes within the EUROfusion Code Development for Integrated Modelling project (WPCD), a simple-to-complex approach has been devised for verification of the European ICRF codes, imported in the European-Integrated Modelling infrastructure, which represents a unique environment for input-data sharing and result analysis. This benchmark activity has been recently extended to non-European codes, in particular the ICRF full-wave `AORSA` code. Here we discussed the results of this benchmark.

Introduction

The main goal of EUROfusion Code Development for Integrated Modelling project (WPCD) [1] is to provide a flexible, modular and integrated suite of codes for preparing and analyzing plasma discharges in view of ITER. This enterprise is based on a three-fold approach: standardise the input and output data of the codes, pursue high level of granularity for flexibility in building workflow, and make the framework suitable for both physics and engineering specifications in order to facilitate an accurate interpretation and prediction of experiments. This has been accomplished with physics/engineering-based hierarchical data structures representing elementary physics problems, called Consistent Physical Object (CPO) [2]. The Universal Access Layer (UAL) software has been developed for transfer of CPOs between modules and the storage system, and it supports Fortran, C++, Python, Java, and Matlab. Finally, the orchestration of complex integrated simulations is achieved with the Kepler graphical workflow environment.
An important ongoing activity on codes ported or implemented in the WPCD framework is *verification*, namely testing whether the implementation accurately represents the claimed physical model, and *validation*, i.e. establishing how accurately the implemented model represents the experiments. In this respect, WPCD offers a unique environment for input-data sharing and data analysis for careful verification of codes addressing the same physical phenomena. Particularly fruitful are those benchmark cases that make possible to isolate and thus to test specific physical mechanisms implemented in the codes. Without manually switching on and off terms in the codes, which is not always numerically feasible or straightforward, this can be sometimes achieved by defining a robust reference scenario and varying pertinent parameters. Additionally, the availability of verification/validation cases with their cleared results is fundamental for *regression testing*, namely testing the changes to modules to guarantee that they do not deteriorate the previous agreement with other codes and experiments.
Having more than one module describing the same physical phenomena is not just desirable for code verification, but adds versatility and longevity to the whole WPCD project. Regarding versatility, in particular, depending on the complexity of the implemented physical model and on the numerical implementation, codes can require quite different computational resources. Therefore, with reference to the final aim in terms of the balance between accuracy and speed, one code can be more suitable than others for a specific workflow.

Radio Frequency Power in Plasmas
AIP Conf. Proc. 1689, 060001-1–060001-4; doi: 10.1063/1.4936499

For what concerns simulation of propagation and absorption of radio-frequency (RF) waves in the ion cyclotron (IC) range of frequencies, WPCD presently counts on four full-wave codes, namely CYRANO [3], EVE [4], LION [5], and TORIC [6]. The ICRF-heating scenarios foreseen in ITER are robust reference cases because of their high single-pass absorption, mainly due to high plasma temperatures and large plasma volumes.
It goes without saying that this benchmark activity is not limited to European codes imported on WPCD infrastructure, although the WPCD framework considerably simplifies its coordination. In fact, in collaboration with PPPL the ICRF full-wave AORSA code [7] recently joined the aforementioned set of ICRF codes in this benchmark activity.
In the next Section we present new cases, which follows from the experience done in the first phase of this activity [9], and discuss the results and outline the future steps in the last Section.

Results

Two main operational phases are foreseen in ITER. In the first, called non-activated (half-field, ≈ 2.65 T on axis) phase, the main ion species is He^4. In the second phase, called activated (only at full-field, ≈ 5.3 T on axis), the main ion species are D and T. The ICRF system can operate with frequencies ranging from ≈ 40 MHz up to ≈ 55 MHz allowing to have $2f_{He^4}$ (≈ 40 MHz for the half-field phase) and $2f_T$ (≈ 53 MHz for the full-field phase) in the plasma core. Since absorption at the second-IC-harmonic resonance is a finite Larmor radius (FLR) effect, whose efficiency increases mainly with the temperature of the resonating species, at least in the initial phase with relatively low plasma temperatures the absorption efficiency is boosted by operating in minority heating (MH) regime with the addition of a few percent of another ion species (minority) with different charge-to-mass ratio with respect to the main ion species (majority). For the two phases in ITER, the minority ion species are H and He^3, respectively. In both cases the fundamental IC resonance of the minority (m) coincides with the second-IC-harmonic of the majority (M), $f_{c\,m} = 2f_{c\,M}$. For the full-field scenario with DT(He^3) plasma the fundamental of D falls inside the plasma on the high-field side. However, the absorption by D ions is weak because of the unfavourable wave polarization and of the "shadow" due to the ion-ion cutoff-resonance (IICR) and $f_{c\,m}$ layers. Finally, electrons compete in absorbing RF power via Landau and transit-time-magnetic-pumping (TTMP) damping, and the higher their temperature is, the more they absorb in the range of temperature and n_φ considered here. By increasing the minority concentration ν_m, the IICR layer moves away from $f_{c\,m}$ towards $f_{c\,M}$ and, roughly speaking, the so-called Mode Conversion (MC) regime replaces the MH one approximately when the IICR layer shifts out from the Doppler-broadened layer around $f_{c\,m}$. In the MC regime the absorption by the minority species weakens in favor of electron absorption, since the wave polarization becomes less favourable and at the ion-ion resonance part of the waves are converted into ion-Bernstein (IBW) and ion-cyclotron (ICW) waves, strongly absorbed by electrons. High resolution is required to numerically resolve IBWs and ICWs, characterized by wavelengths much shorter than those of the launched fast waves. An increase of ν_m causes also a widening of the IICR evanescence layer between the cutoff on the low-field side (LFS) and the ion-ion resonance on the high-field side (HFS) where MC occurs. These two effects determines an optimum of ν_m for MC regime.

These are the two reference scenarios considered in this benchmark activity, whose results in its initial phase showed good agreement in the trends of the global RF-power repartition but also some quantitative discrepancies [9]. Moreover, discrepancies were observed in the position of the peaks of the RF-power deposition profiles. To pin down the causes of these differences, it has been decided to follow a simple-to-complex approach by starting with circular equilibria (even with unrealistic reduced Grad-Shafranov shift) of the same size of the final realistic ones. Incidentally, all the equilibria considered in this activity are generated with the equilibrium CHEASE code [8].

Table 1. ICRF benchmark cases.

Shot/Run	Scenario	Geometry	frequency	$f_{c\,m}$
40/1	half-field	circular	35 MHz	LFS
40/2	half-field	circular (red. GS shift)	35 MHz	LFS
40/3	half-field	circular	36.8 MHz	on-axis
40/4	half-field	circular	42 MHz	HFS
40/11	half-field	elliptic	35 MHz	LFS
50/1	full-field	circular	48 MHz	LFS

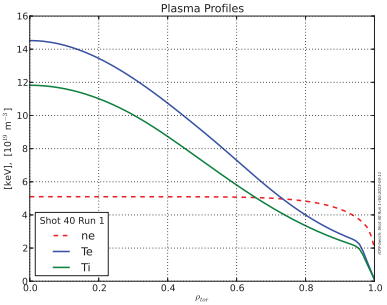

A WPCD dataset can be organized as an experimental shotfile, i.e. as an array of CPOs with the array index working as a time counter. In the present case, the shotfiles are created with loops over varied parameters, and the inmost one is over the minority concentration ν_m. In both scenarios, we have considered ten equispaced values of ν_m

starting from 2% up to 20%. Especially in the case of He^3 in ITER, it sounds economically unrealistic to have ν_m above a few percent, but it is useful to extend the ν_m scan to test the transition from MH to MC regimes. The second varied parameter is the electron temperature (T_e) which is halved and doubled. This is useful to test the electron Landau and TTMP damping. Next, the ion temperature (T_i) of He^4 and T, respectively, are also halved and doubled to test the IC harmonic calculations. Finally, the last loop is on the toroidal wavenumber, and precisely {27, 50}, which has a strong impact on both wave propagation and absorption. Each shot file is made of 180 time slices, and they differ at least for either frequency or equilibrium. The frequency is varied to have f_{cm} on the LFS, close to the magnetic axis, and on the HFS. One of the effects of shifting f_{cm} towards the HFS is to increase the plasma volume between the antenna and the f_{cm}-resonance layer with the result of increasing the faction of RF power absorbed by electrons. Table 1 summarizes the shotfiles so far considered together with the reference plasma profiles for half-field scenarios. The absorbed RF power is 10 MW.

Figure 1 shows the power repartition as function of H concentration for the nominal plasma profiles in the case of circular (40/1) on the left and elliptic (40/11) equilibria on the right. The higher minority absorption and the lower electron absorption in 40/11 w.r.t 40/1 is likely due to the larger volume due to ellipticity.

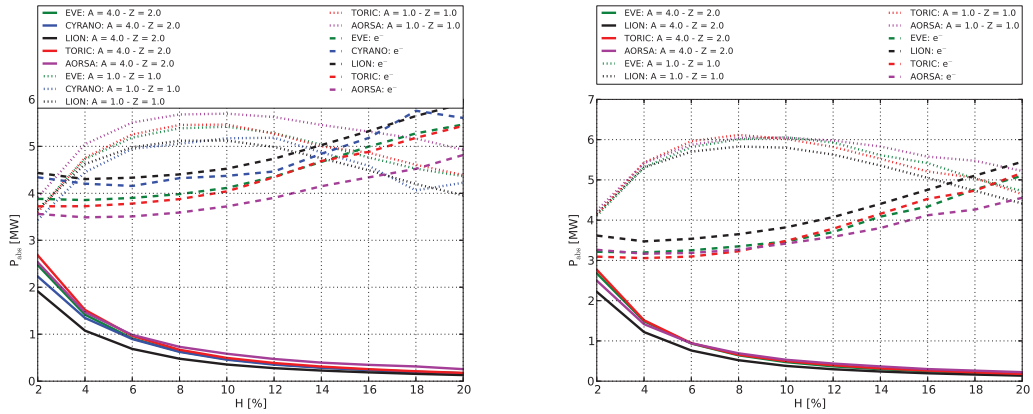

FIGURE 1. Power repartition for the first ten time slices of circular 40/1 (left) and elliptic 40/11 (right) cases.

These two cases are representative of the quality of the agreement so far achieved: The trends with the minority concentration predicted by the five codes agree reasonably well and the agreement improves for those cases characterized by low electron absorption. In particular, the effect of electron absorption is clear in figure 2 which shows the power repartition for 40/1 with halved (left) and doubled (right) T_e.

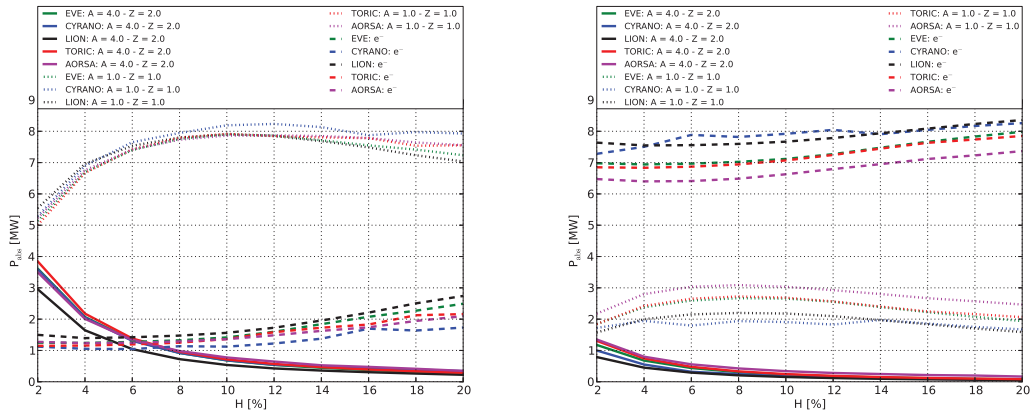

FIGURE 2. Power repartition of 40/1 for halved (left) and doubled (right) T_e.

Figure 3 shows the deposition profiles for 40/1 corresponding to the point at 6% of H concentration, shown in

figure 1(left). Compared with the previous results [9], now all codes agree on the position and width of the peak of the deposition profiles, although there are still some discrepancies on the amplitudes.

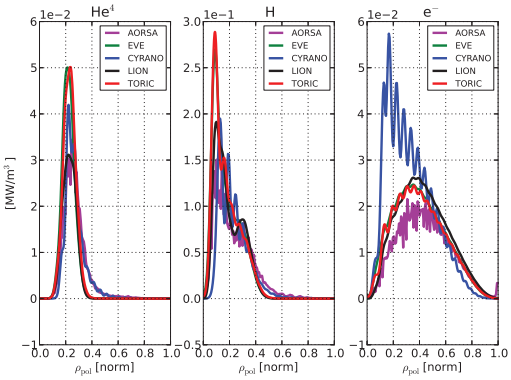

FIGURE 3. Power deposition profiles of shot 40/1 with 6% of H and nominal plasma profiles.

Discussion and conclusions

After [9], the combined electron Landau&TTMP damping of the fast wave, valid for arbitrary direction of propagation, has been consistently introduced in `LION`. As a consequence, now `LION` results are much closer to those of the other codes. Also the quantitative agreement between `EVE` and `TORIC` is improved making the differences almost imperceptible. This general improvement of the agreement has been achieved also with a careful tuning/checking of the input data read from CPOs, made possible by the simpler equilibria considered here. The results of `CYRANO` code are closer to those of the other codes when $\approx 20\%$ reduced n_φ value is used. This issue is presently under investigation with a close comparison with the other codes. From the cases so far considered, the agreement worsens when the electron absorption is high. Precisely, `EVE` and `TORIC` are still in a very good agreement, but their results slightly move away from those of `AORSA` and `LION`. This is likely due to the different implementation of electron damping in `LION` and `AORSA` with respect to `EVE` and `TORIC`, and will be investigated in the near future.

Acknowledgments

We thank the EU-Integrated Modelling (EU-IM) Contributors (WPCD and WPISA-CPT), and, in particular, G.Falchetto and D.Coster for their continuos support.

This work has been carried out within the framework of the EUROfusion Consortium and has received funding from the Euratom research and training program 2014-2018 under grant agreement No 633053. The views and opinions expressed herein do not necessarily reflect those of the European Commission. This work was supported by SciDAC Center for Wave-Plasma Interactions under DE-FC02-01ER54648 and the US DOE under DE-AC02-CH0911466. This research used resources of the National Energy Research Scientific Computing Center, a DOE Office of Science User Facility supported by the Office of Science of the U.S. Department of Energy under Contract No. DE-AC02-05CH11231.

REFERENCES

[1] G. Falchetto et al., *Nuclear Fusion* **54**, 043018 (2014).
[2] F. Imbeaux,et al. *Comp. Phys. Comm.*, 181(6):987 – 998, (2010).
[3] P. U. Lamalle, PhD thesis - Université de Mons (1994) LPP-ERM/KMS Laboratory Report 101.
[4] R. Dumont, *Nuclear Fusion* **49**, 075033 (2009).
[5] L. Villard, S. Brunner, and J. Vaclavik, *Nuclear Fusion* **35**, 1173 (1995).
[6] M. Brambilla and R. Bilato, *Nuclear Fusion* **46**, S387 (2006).
[7] E. F. Jaeger, L. A. Berry, E. D'Azevedo et al, *Physics of Plasmas* **8**, 1573 (2001).
[8] H. Lütjens, A. Bondeson, and O. Sauter, *Computer Physics Communications* **97**, 219 (1996).
[9] R. Bilato et al.,*AIP Conference Proceedings* **1580**, 291 (2014).